

## Neutron-diffraction study of the metamagnetic phases in $\text{HoNi}_2\text{B}_2\text{C}$

A. J. Campbell and D. McK. Paul

*Department of Physics, University of Warwick, Coventry, CV4 7AL, United Kingdom*

G. J. McIntyre

*Institut Laue-Langevin, Boîte Postale 156, 38042 Grenoble Cedex 09, France*

(Received 1 April 1999)

Neutron diffraction has been used to determine the magnetic phase diagram of  $\text{HoNi}_2\text{B}_2\text{C}$ , in the plane of temperature and magnetic field up to 4.6 T, for two different crystallographic orientations relative to the applied magnetic field. For both orientations two first-order metamagnetic transitions are observed below 5.5 K as the applied field is increased. In both cases the first transition is to a state in which the magnetic structure is modulated along the  $c$  axis with wave vector  $\delta=[0,0,0.667]$ . With the field applied parallel to the  $[1\bar{1}0]$  direction the second transition is to a saturated paramagnetic state in which the spins are aligned ferromagnetically by the applied magnetic field. With the field parallel to the  $[0\ 1\ 0]$  direction, the second transition is into a state in which the magnetic structure is modulated along the  $b$  axis with wave vector  $\delta=[0,0.610,0]$ , in disagreement with a simplified theoretical model.

The family of superconducting compounds of the form  $\text{RNi}_2\text{B}_2\text{C}$  ( $R$ =rare earth) have been the subject of considerable investigation since their discovery.<sup>1-4</sup> Of particular interest are those members of the family that contain magnetic rare-earth ions (such as Er, Ho, Dy) as they have provided an opportunity to study the interplay between magnetism and superconductivity. This interplay can result in unusual effects. For example, in  $\text{DyNi}_2\text{B}_2\text{C}$  it appears that the hysteresis in one of the metamagnetic transitions at temperatures below 2 K results in re-entrant behavior for the superconductivity.<sup>5</sup> The magnetic properties of these materials have been found to be extremely anisotropic.<sup>6</sup> In  $\text{HoNi}_2\text{B}_2\text{C}$  the crystalline electric field (CEF) splitting of the ground-state multiplet of the  $\text{Ho}^{3+}$  ion means that below the magnetic ordering temperature the magnetic moment is essentially confined to the basal ( $a$ - $b$ ) plane.

$\text{HoNi}_2\text{B}_2\text{C}$  has proved to be one of the most interesting of these compounds. It has a superconducting transition at around 9 K but between 7 and 5 K  $H_{c2}$  is dramatically lowered. Neutron-diffraction measurements<sup>7</sup> have shown that below 8.5 K there is a transition to an incommensurate spiral antiferromagnetic state with a modulation along the  $c$  axis of 136 Å. However, between 7 and 5 K, where the superconductivity is suppressed there is an additional modulation along the  $a$  axis. A recent investigation<sup>11</sup> of the flux profiles in  $\text{HoNi}_2\text{B}_2\text{C}$  has shown that bulk pinning of the flux-line lattice only becomes significant when this additional modulation is present, showing the influence of the magnetism on the superconductivity. Below 5 K there is a further transition to a commensurate antiferromagnetic state. This consists of ferromagnetic planes coupled antiferromagnetically along the  $c$  axis. In addition to the anisotropy between in-plane and out-of-plane properties there is also anisotropy within the basal plane. Further evidence of this anisotropy comes from the critical-field values of two metamagnetic phase transitions which have been observed at 2 K with a magnetic field applied perpendicular to the  $c$  axis. Canfield *et al.*<sup>8</sup> measured the angular dependence of these transitions at 2 K by mag-

netization measurements and found a third transition for certain orientations of the sample relative to the applied field. Based on their data they have proposed possible net distributions of the magnetic moments for the different phases. Here we present initial results from an ongoing series of neutron-diffraction measurements to determine the magnetic structure of these various phases both in  $\text{HoNi}_2\text{B}_2\text{C}$  and other members of the  $\text{RNi}_2\text{B}_2\text{C}$  series. Neutron diffraction is the ideal technique for such studies as it allows a direct measurement of magnetic modulations whereas magnetization experiments only allow measurement of the net moment along the direction of the applied field.

The sample used in our experiment is a single crystal of  $\text{HoNi}_2\text{B}_2\text{C}$  grown using a  $\text{Ni}_2\text{B}$  flux technique which has been well documented elsewhere.<sup>6,7</sup> The boron isotope  $\text{B}^{11}$  was used to reduce neutron absorption. Magnetization measurements were carried out as a function of temperature and field using a vibrating sample magnetometer. These showed that our sample had transition temperatures in good agreement with those reported<sup>8,9</sup> and confirmed the presence of the metamagnetic transitions below 5.5 K. Neutron-diffraction measurements were carried out on the thermal neutron normal-beam diffractometer, D15, of the reactor source at the Institut Laue-Langevin, in Grenoble, France. D15 has a Cu monochromator and the  $[3\ 3\ 1]$  reflection was used, giving an incident wavelength of 1.17 Å.

The sample was mounted in a 4.6-T vertical cryomagnet and two sample orientations were used in order to investigate all the metamagnetic phases in this field range. The phase diagrams were mapped out by following the peak intensity of a weak fundamental reflection as a function of field at constant temperature, to detect the net ferromagnetic component at each metamagnetic transition. Within each phase we made scans along various reciprocal-space directions to detect possible antiferromagnetic modulations. A characteristic reflection of each modulation observed was also followed as a function of field to confirm the location of the phase boundaries. A temperature scan was performed on a reflection

characteristic of each phase, in both the increasing and decreasing field cycles, to establish the temperature phase boundaries. Finally, most accessible commensurate, and, where appropriate, incommensurate, reflections were scanned at fixed conditions in each phase to allow accurate refinement of the nuclear and magnetic structures. Full details of the structural refinements will be presented elsewhere; here we give just the principal results.

Initially the sample was mounted with the  $[1\bar{1}0]$  crystallographic direction parallel to the magnetic field. Scans above the magnetic ordering temperature showed that the sample was of excellent quality and, as expected, had a body-centered tetragonal structure (space group  $I4/mmm$ ) resulting in nuclear reflections at  $h+k+l=2n$  reciprocal-lattice points only. Measurements to determine the zero-field magnetic structures were then made, and were in agreement with those previously reported.<sup>12</sup> Below 8.5 K satellites were observed in the  $c^*$  direction corresponding to a modulation along the  $c$  axis with wave vector  $\delta=[0,0,0.081]$ . An additional modulation along the  $a$  axis has a wave vector  $\delta=[0.583,0,0]$  as previously observed.<sup>7</sup> The intensity of one such satellite was followed in temperature and confirmed the presence of this modulation between 5.5 and 7 K. Below 5.5 K there is a transition to an antiferromagnetic state in which the moments are coupled antiferromagnetically along the  $c$  axis and ferromagnetically, along  $[1\ 1\ 0]$ -type directions, in the  $a$ - $b$  plane. The sample was then cooled to 2 K and the intensity of the  $[1\ 1\ 0]$  peak was followed as a function of field. Metamagnetic transitions were observed at around 0.5 and 1.2 T as the field was increased, as shown in Fig. 1(a). There is a large hysteresis in these transitions, showing their first-order nature. Several such field sweeps were performed at different temperatures in order to map out the phase diagram shown in Fig. 1(b).

Having established the phase boundaries the field was set to 0.75 T (at 3 K), in the region marked II on the phase diagram. Additional peaks were observed in the  $c^*$  direction at positions  $h, k, l \pm 0.667$  ( $h+k+l=2n$ ). This modulation, combined with the ferromagnetic component corresponds to a repeating sequence along the  $c$  axis of two spins parallel to  $[1\bar{1}0]$  and one antiparallel to  $[1\bar{1}0]$ . Next the field was set to 1.5 T (at 3 K) which is in region III of the phase diagram. We found no evidence of antiferromagnetic modulations in this phase. However the fundamental nuclear reflections did exhibit a large increase in intensity on entering this phase as illustrated by Fig. 1(a). Thus the spins are simply aligned ferromagnetically in the  $[1\bar{1}0]$  direction. The two structures observed in a field applied along the  $[1\bar{1}0]$  direction below 5.5 K agree with the predictions of Canfield *et al.*<sup>8</sup>

The sample was then realigned in the cryomagnet with the  $[0\ 1\ 0]$  crystallographic direction parallel to the field. The sample was cooled to 2 K, at which temperature the intensity of the  $[1\ 0\ 1]$  reflection was measured as a function of magnetic field. This is shown in Fig. 2(a) and clearly shows metamagnetic transitions at 0.7 and 0.96 T as the field is increased. Both transitions are again first order and show a large hysteresis. Several such field sweeps were performed in order to establish the magnetic phase diagram, in the plane of temperature and magnetic field, for this orientation of the crystal relative to the magnetic field. The phase diagram is

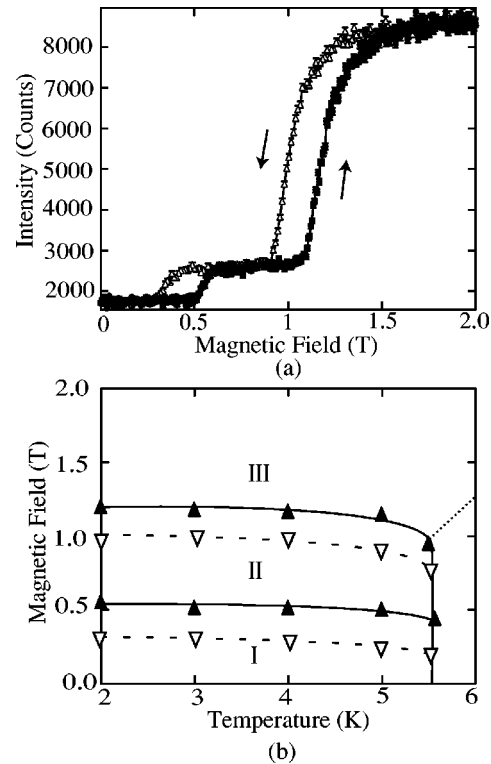


FIG. 1. (a) The intensity of the  $[1\ 1\ 0]$  reflection versus applied magnetic field at 2 K, with the field applied along the  $[1\ 1\ 0]$  crystallographic direction. The field increasing data clearly shows metamagnetic transitions at 0.5 and 1.2 T. Both transitions are hysteretic, showing their first-order nature. (b) Magnetic phase diagram of  $\text{HoNi}_2\text{B}_2\text{C}$  with the magnetic field applied parallel to the  $[1\ 1\ 0]$  crystallographic direction. The triangles indicate the direction of the field sweep. The phases I, II, and III are described in the text. The dotted line represents the boundary between this phase and the incommensurate antiferromagnetic state. This boundary was not established in these measurements. The solid and dashed lines are a guide to the eye.

shown in Fig. 2(b). At 7 K a field scan up to 4 T revealed no evidence for the onset of the phase marked IV on the phase diagram. It seems likely that above 6.5 K the phase boundary for this phase becomes very steep. In zero field the temperature was set to 3 K. The field was then set to 0.75 T, i.e., in the phase marked II on the phase diagram. This phase was expected to have the same modulation as the phase II in the set of measurements with the  $[1\bar{1}0]$  parallel to the field. A  $q$  scan in the  $c^*$  direction confirmed that this was the case. The field was then set to 1.5 T (still at 3 K) so that the sample was in the region marked IV on the phase diagram. Here, extra reflections were observed in the  $b^*$  direction only, at positions  $h, k \pm 0.61, l$  ( $h+k+l=2n$ ). Structure refinements against the intensities of the incommensurate reflections show that these peaks arise from a modulation in the  $a$  axis component of the moment. This modulation, combined with the ferromagnetic component along the  $b$  axis, corresponds to an alternating herringbone pattern of spins along  $[1\ 1\ 0]$  and  $[1\bar{1}0]$ . Interestingly, the wave vector of the modulation is close to the  $a$  axis (or equivalently  $b$  axis) modulation with wave vector  $\delta=[0.583,0,0]$  that is observed in zero field. Only the first of the two structures observed in a field applied parallel to the  $[0\ 1\ 0]$  direction below 5.5 K agree with the

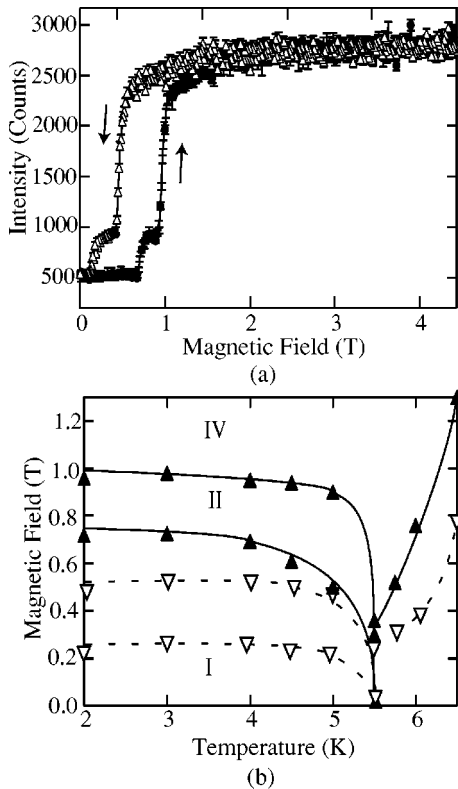


FIG. 2. (a) Intensity of the  $[1\ 0\ 1]$  reflection versus applied magnetic field at 2 K with the field applied parallel to the  $[0\ 1\ 0]$  crystallographic direction. The field increasing data clearly show metamagnetic transitions at 0.7 and 0.96 T. Both transitions are first order and show a large hysteresis. (b) Magnetic phase diagram of  $\text{HoNi}_2\text{B}_2\text{C}$  with the field applied parallel to the  $[0\ 1\ 0]$  crystallographic direction. The triangles indicate the direction of the field sweep. The phases I, II, and IV are described in the text. The three phases are marked for the field increasing measurements. The solid and dashed lines are guides to the eye.

predictions of Canfield *et al.*<sup>8</sup> The limit of 4.6 T of our cryomagnet prevented us from observing the third transition, presumably to a purely ferromagnetic phase.

We can compare the results with the model of Amici and Thalmeier<sup>10</sup> for the magnetic phase transitions in this material. They applied a mean-field treatment to the problem, which is simplified by ignoring the  $a$ -axis modulation (so that all the phases are ferromagnetically coupled in the basal plane) and ignoring any small  $c$ -axis component of the magnetic moment. From the magnetization data of Canfield *et al.*,<sup>8</sup> Amici and Thalmeier argued that the magnetic moments of the ions must be almost at saturation value and that they must be locked in one of the four equivalent in-plane  $[1\ 1\ 0]$ -type directions. This gives rise to six possible structures. All the structures can be represented by a repeating sequence of six moments along the  $c$  axis. This means that the interaction of the system only has four free parameters,  $j_i$  for  $i=0,1,2,3$ .  $j_0$  represents the in-plane interactions and the

other terms represent interactions with the moments in other layers. Magnetization curves, calculated using these parameters, were used to construct the phase diagram. For more details the reader is referred to the original paper. With the field applied parallel to the  $[1\bar{1}0]$  crystallographic direction the proposed phase boundaries and magnetic structures agree well with our results. With the field applied parallel to the  $[0\ 1\ 0]$  crystallographic direction the phase boundaries again agree well with those observed. The magnetic structure of phase II is also correctly predicted. However, in phase IV the model again predicts a magnetic structure modulated along the  $c$  axis when in fact it is modulated along the  $b$  axis. The condition, imposed in the model, of ferromagnetism in the  $a$ - $b$  plane means only  $c$ -axis modulations can be predicted to occur. Our results show that this assumption is not valid and a two component model is required. The model also predicts the occurrence of two other phases that are not observed experimentally. It is clear from other experiments<sup>7,11</sup> that there is an interaction between the magnetism and the superconductivity and a correct description of the magnetic ordering in a field may also require the influence of both components. The occurrence of the phase modulated along the  $b$  (or equivalently  $a$ ) axis is particularly interesting. In zero field the  $a(b)$ -axis modulation is observed in addition to the  $c$ -axis modulation over a finite temperature range. It is not clear whether or not these two modulation coexist macroscopically or in separate domains.<sup>12</sup> Either way they must be similar in energy and our results show that the application of a field favors the  $a(b)$ -axis modulation and the  $c$ -axis modulation disappears.

Neutron diffraction has been used to establish the magnetic phase diagram of  $\text{HoNi}_2\text{B}_2\text{C}$  for two different orientations of the applied magnetic field relative to the crystal. For both orientations the sample undergoes two metamagnetic transitions as the applied field is increased. The field at which the transitions occur is strongly dependent on the orientation of the sample relative to the applied magnetic field showing that there is considerable anisotropy even within the  $a$ - $b$  plane. In both cases the first transition is into a state in which the magnetic structure is modulated along the  $c$  axis with wave vector  $\delta=[0,0,0.667]$ . With the field applied parallel to the  $[1\bar{1}0]$  crystallographic direction the second transition is into a saturated paramagnetic state in which the spins are held parallel by the applied field. However, with the field applied parallel to the  $[0\ 1\ 0]$  crystallographic direction the second transition is into a state in which the magnetic structure is modulated along the  $b$  axis with wave vector  $\delta=[0,0.610,0]$ . This is similar to the  $a(b)$ -axis modulation that coexists with the  $c$ -axis modulation in zero field. The application of a field apparently favors the  $b$ -axis modulation.

Work is currently in progress performing similar measurements on  $\text{ErNi}_2\text{B}_2\text{C}$ ,  $\text{DyNi}_2\text{B}_2\text{C}$ , and other rare-earth nickel borocarbides.

- <sup>1</sup>R. Nagarajan *et al.*, Phys. Rev. Lett. **72**, 274 (1994).  
<sup>2</sup>R. J. Cava *et al.*, Nature (London) **367**, 252 (1994).  
<sup>3</sup>T. Siegrist *et al.*, Nature (London) **367**, 254 (1994).  
<sup>4</sup>R. J. Cava *et al.*, Nature (London) **367**, 146 (1994).  
<sup>5</sup>Z. Q. Peng *et al.*, Phys. Rev. B **57**, R8123 (1998).  
<sup>6</sup>For example, B. K. Cho *et al.*, Phys. Rev. B **52**, 3684 (1995).  
<sup>7</sup>C. V. Tomy *et al.*, Physica B **213-214**, 139 (1995).  
<sup>8</sup>P. C. Canfield *et al.*, Phys. Rev. B **55**, 970 (1997).  
<sup>9</sup>B. K. Cho *et al.*, Phys. Rev. B **52**, 3684 (1995).  
<sup>10</sup>A. Amici and P. Thalmeier, Phys. Rev. B **57**, 10 684 (1998).  
<sup>11</sup>C. D. Dewhurst *et al.*, Phys. Rev. Lett. **82**, 827 (1999).  
<sup>12</sup>J. W. Lynn *et al.*, Phys. Rev. B **55**, 6584 (1997).